Charge Transport and Magnetism in $Tm_{0.03}Yb_{0.97}B_{12}$

V. Glushkov[a,*], A. Azarevich[a], M. Anisimov[a], A. Bogach[a], S. Demishev[a],
A. Dukhnenko[b], V. Filipov[b], K. Flachbart[c], S. Gabáni[c], S. Gavrilkin[d], M. Kondrin[e],
N. Shitsevalova[b] and N. Sluchanko[a]

[a]Prokhorov General Physics Institute of RAS, Vavilov Str. 38, 119991 Moscow, Russia
[b]Frantsevich Institute for Problems of Materials Science, NAS, Krzhyzhanovsky Str. 3, 03680 Kiev, Ukraine
[c]Institute of Experimental Physics, SAS, Watsonova 47, 040 01 Košice, Slovakia
[d]Lebedev Physical Institute of RAS, Leninskii pr. 53, 119991 Moscow, Russia
[e]Vereshchagin Institute of High Pressure Physics of RAS, Troitsk, 142190 Moscow, Russia

Transport and magnetic properties of polycrystalline $Tm_{0.03}Yb_{0.97}B_{12}$ samples were investigated at temperatures 1.8–300 K in magnetic fields up to 9 T. The activated behavior of resistivity, the Hall coefficient and thermopower is described in terms of a narrow gap $\varepsilon_g \approx 16.6$ meV, which controls the charge transport in $Tm_{0.03}Yb_{0.97}B_{12}$ at $T > 40$ K. The maximum of magnetic susceptibility found at 50 K is shown to be induced by a spin gap $\Delta \approx 4.7$ meV being close to the half of the spin fluctuation energy in YbB_{12}. Large diffusive thermopower $S = AT$, $A = -29.1$ μV/K^2 and the Pauli susceptibility $\chi_0 \approx 7.2 \times 10^{-3}$ emu/mol found below 20 K seem to be associated with the many-body resonance, which corresponds to states with an enhanced effective mass $m^* \approx 250 m_0$ (m_0 — free electron mass). The effective parameters of magnetic centers and the analysis of anomalies favor the nonequivalent states of substitute Tm ions.

1. Introduction

The nature of the narrow gap ($\varepsilon_g \approx 17.8$ meV [1, 2]) in YbB_{12}, which shares the place between antiferromagnetic metal TmB_{12} [3] and superconducting LuB_{12} [4] in the set of rare-earth dodecaborides RB_{12}, stays a subject of discussions [1–3, 5–11]. The ground state of YbB_{12} identified usually as the Kondo insulator [1] seems to have a non-trivial topology of the band structure resulting in surface conductivity [5]. However, studies of Lu-doped and Zr-doped YbB_{12} show that the gap in the YbB_{12} band spectrum is local and is not influenced by the onset of long-range coherence [6, 7]. Recent studies of $Tm_xYb_{1-x}B_{12}$ single crystals [8–10] pointed out that the rise of Yb content results in a metal–insulator transition, a bulk narrow many-body resonance ($\Delta \approx 6$ meV) appears at the Fermi level. The band spectrum renormalization seen from the thermopower enhancement (from $S = -2$ μV/K for TmB_{12} up to $S = -230$ μV/K for $Yb_{0.81}Tm_{0.19}B_{12}$ [8]) is suggested to be induced by the Yb^{3+}–Yb^{3+} dimer formation. This assumption may be proved by a study of Yb-rich samples ($x < 0.19$), which were not available for the transport studies up to now [9–11].

2. Experimental methods

To shed more light on the nature of the ground state of such a system, transport and magnetic properties of the

---

*corresponding author; e-mail: glushkov@lt.gpi.ru

$Tm_{0.03}Yb_{0.97}B_{12}$ substitutional solid solution were studied. High purity polycrystalline $Tm_{0.03}Yb_{0.97}B_{12}$ samples were grown by crucibleless inductive zone melting in argon atmosphere. Any secondary phases were excluded by X-ray diffraction analysis. The real thulium content in the solid solution estimated from EPMA study ($x \approx 0.04$) was found to exceed slightly the nominal one. A five probe method was used to measure resistivity and Hall effect at temperatures 2–300 K in magnetic fields up to 8.2 T. The Seebeck coefficient was studied at temperatures 3–300 K by the original 4-probe technique with a step-by-step temperature gradient sweeping at fixed temperature [8]. The temperature and field dependences of magnetization were measured with the help of Quantum Design PPMS-9 setup.

3. Results and discussion

Transport properties of $Tm_{0.03}Yb_{0.97}B_{12}$ are summarized in Fig. 1. Lowering of temperature results in a monotonous increase of resistivity (Fig. 1a), which changes from $\rho(300$ K$) \approx 440$ $\mu\Omega$ cm to $\rho(2$ K$) \approx 9.6$ mΩcm. The large inverse resistivity ratio IRR $= \rho(2$ K$)/\rho(300$ K$) \approx 22$ as compared to IRR ≈ 9.3 for $Tm_{0.19}Yb_{0.81}B_{12}$ single crystal [9] proves the high quality of samples under investigation. At $T > 100$ K the resistivity is well described by the thermal activation law $\rho \sim \exp(-E_R/T)$ with a characteristic energy $E_R \approx 75.3$ K. The E_R value is considerably lower than those ones estimated for the Hall constant ($E_H \approx 96.7$ K) and the Seebeck coefficient ($E_S \approx 173$ K). The E_H value gives a correct estimation of the gap size in $Tm_{0.03}Yb_{0.97}B_{12}$ ($\varepsilon_g = 2E_H \approx 16.6$ meV). The same signs of the Hall and

Seebeck effects (Fig. 1c,d) prove the major electron contribution to charge transport while the negative magnetoresistance $\Delta\rho/\rho = (\rho(H) - \rho(0))/\rho(0)$ points to a dominant magnetic scattering of charge carriers. However, the discrepancy between the E_H and E_S values ($E_H < E_S$) cannot be explained by the difference between the mobilities of holes and electrons in the intrinsic semiconductor model.
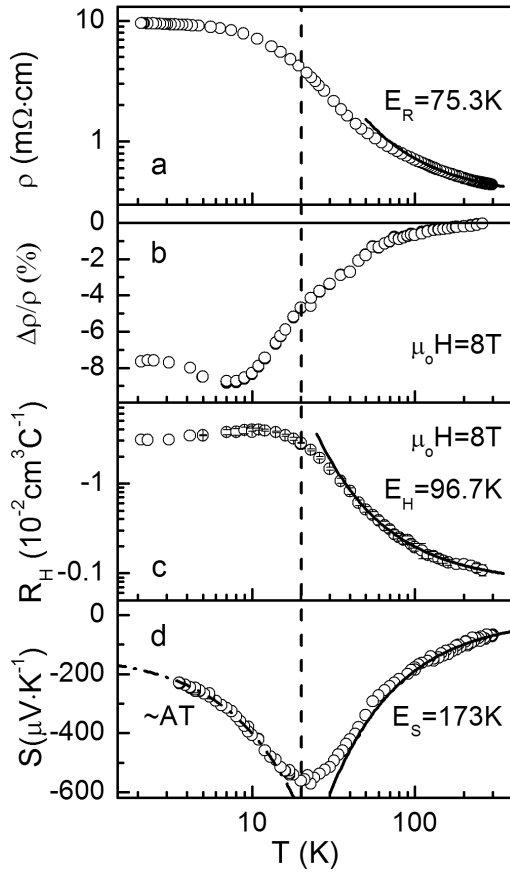

Fig. 1. Resistivity ρ (a), magnetoresistance $\Delta\rho/\rho$ (b), the Hall constant R_H (c) and thermopower S (d) of $Tm_{0.03}Yb_{0.97}B_{12}$. Solid lines correspond to the activation asymptotics (see text). The dash-dotted line in part (d) shows the linear $S(T)$ fit with $A = -29.1\ \mu V/K^2$. The vertical dashed line marks the position of $S(T)$ minimum (see also Fig. 3).

The saturation of resistivity and Hall constant below 10 K (Fig. 1a,c) is followed by an emergent feature of thermopower, which passes through a minimum $S \approx -560\ \mu V/K$ at $T = 20$ K and rises as $S \sim AT$ with $A = -29.1\ \mu V/K^2$ when temperature decreases (Fig. 1d). The extreme value of the Hall constant at $T \approx 10$ K (Fig. 2c) appears due to contribution from the anomalous Hall effect identified clearly from the field dependences of the Hall resistivity. This contribution does not exceed 5.6 $\mu\Omega$ cm and will be discussed elsewhere.

The temperature dependence of the magnetic susceptibility calculated from $M(T, 0.1T)$ magnetization data as $\chi = M/H$ shows a non-monotonous behavior with low-temperature upturn (Fig. 2a). At $T > 40$ K the $\chi(T)$ data can be well fitted by the spin gap model $\chi_S(T) = \chi_{S0} + C_S/T \exp(-\Delta/T)$ applied earlier for the relative compound SmB_6 [12]. The spin gap size $\Delta \approx 54.7$ K is approximately equal to the half of the spin fluctuations temperature in YbB_{12} ($T_{sf} \approx 100$ K) [11] and is comparable with the binding energies of in-gap many-body states ($E_a = 65 \pm 10$ K) detected in $Tm_{1-x}Yb_xB_{12}$ ($x < 0.19$) [9]. The Curie constant $C_s \approx 1.77$ emu K/mol corresponds to the effective moment $\mu_{eff} \approx 3.8\ \mu_B$ (μ_B — Bohr magneton), which is considerably lower than the respective free Yb^{3+} ion value $\mu_{eff} \approx 4.5\ \mu_B$.

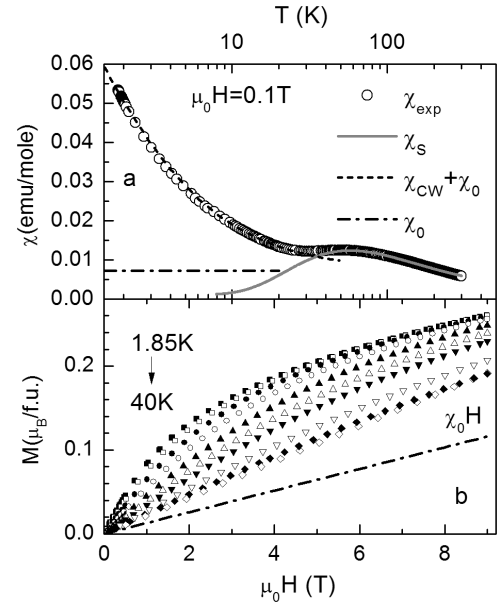Fig. 2. (a) Molar susceptibility $\chi(T)$ of $Tm_{0.03}Yb_{0.97}B_{12}$ calculated from the $M(T, 0.1T)$ magnetization data. Solid and dashed lines represent the fits within spin gap and the Curie–Weiss models (see text). (b) Isothermal magnetization $M(H, T_0)$ of $Tm_{0.03}Yb_{0.97}B_{12}$ measured at $T_0 = 1.85$, 2.3, 3.1, 4.2, 6, 8, 10, 15, 20, and 40 K. Dash-dotted lines in parts (a) and (b) show the contributions from low-temperature Pauli susceptibility $\chi_0 \approx 7.2 \times 10^{-3}$ emu/mol.

Below 20 K magnetic susceptibility follows the Curie–Weiss law $\chi_{CW} = C_0/(T - \Theta)$ with $C_0 \approx 0.13$ emu K/mol and $\Theta \approx -1.0$ K, which is biased by the temperature independent contribution $\chi_0 \approx 7.2 \times 10^{-3}$ emu/mol (Fig. 2a). The $\chi_0 H$ term agrees well with the high field trend of the $M(H, T < 4$ K) data (Fig. 2b). The correct estimation of χ_{CW} and χ_0 is also proved by the scaling of saturated magnetization $M - \chi_0 H$ as a function of $H/(T - \Theta)$ being valid for $T < 20$ K (not shown here). Note that a similar procedure has been successfully applied to separate different contributions to the magnetization of the $Tm_{1-x}Yb_xB_{12}$ solid solutions for $x < 0.19$ [10]. The straightforward calculation for $Tm_{0.03}Yb_{0.97}B_{12}$ results in the saturated moment $\mu_S \approx 7.3\ \mu_B$ and the effective concentration of centers $N_0 \approx 0.02$ (per formulae unit).

The correlated behavior of transport and magnetic properties for Yb-rich dodecaborides can be clearly established from the temperature behavior of the difference $\chi(T) - \chi_{CW}(T)$ (Fig. 3a) and from effective parameters of charge carriers (Fig. 3b,c). Indeed, the electron concentration estimated from the Hall constant as $n = (R_H e)^{-1}$ can be well fitted by the combination of a thermally activated contribution $n(T)/n_{RE} = n_1 \exp(-E_H/T)$ with $n_{RE} = 9.6 \times 10^{21}$ cm^{-3} and $n_1 = 0.92$ and a temperature independent addition $n_0 = 0.016$ per rare-earth ion (Fig. 3c). The crossover temperature $T_0 \approx 20$ K matches perfectly the positions of the electron mobility maximum (Fig. 3b) and the maximal amplitude of the Seebeck effect (Fig. 1d). Besides, the $\Delta\chi = \chi(T) - \chi_{CW}(T)$ contribution increases rapidly below T_0 approaching the estimated χ_0 value (Fig. 3a).
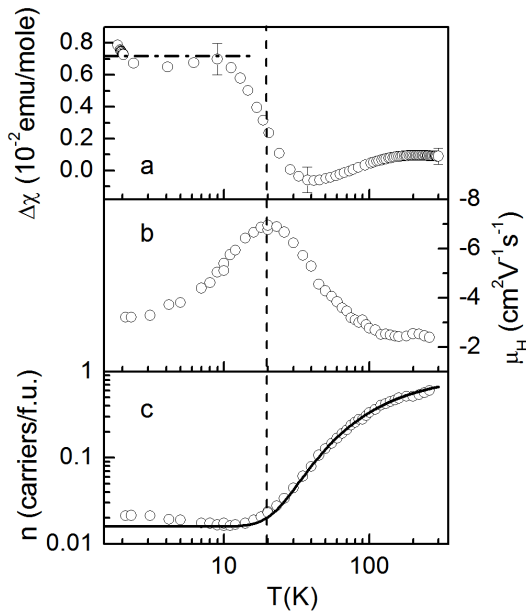

Fig. 3. The difference $\Delta\chi = \chi(T) - \chi_{CW}(T)$ (a), the Hall mobility μ_H (b), and concentration of charge carriers per formula unit n (c) in $Tm_{0.03}Yb_{0.97}B_{12}$. The dash-dotted line in part (a) shows the value of χ_0 (see caption to Fig. 2). The solid line in part (c) corresponds to the $n(T)/n_{RE} = n_0 + n_1 \exp(-E_H/T)$ fit with $n_0 = 0.016$ and $n_1 = 0.92$. The vertical dashed line marks the position of $|\mu_H(T)|$ maximum (see also Fig. 1).

In our opinion, the low temperature anomalies of charge transport and magnetic properties of $Tm_{0.03}Yb_{0.97}B_{12}$ can be well understood in terms of a temperature induced transformation of the band spectrum discussed earlier in [8–10]. Indeed, a straightforward calculation of the density of states at the Fermi level using standard expressions for diffusive thermopower AT and the Pauli susceptibility χ_0 results in $N(\varepsilon_F) \approx 4.9 \times 10^{35}$ erg^{-1} cm^{-3} and $N(\varepsilon_F) \approx 5.7 \times 10^{35}$ erg^{-1} cm^{-3}, respectively. Within the single electron model these values correspond to an extremely large effective mass of charge carriers $m^* \approx 250 m_0$. The estimated relaxation time $\tau = m^* \mu_H/e \approx 0.6$ ps agrees well with inverse valence fluctuation rate $\tau \approx 0.4$ ps estimated from optical and neutron studies [2, 11]. Finally, the very good correlation between the sum $N_0 + n_0 \approx 0.036$ and the Tm concentration (≈ 0.04) favors the nonequivalent states of substitute ions, which may appear due to their various positions in respect of the ytterbium dimers [9, 10]. However, an extended study of the $4f$–$5d$ hybridization effects in Yb-rich compounds is required to prove this suggestion.

Acknowledgments

References

[1] F. Iga, N. Shimizu, T. Takabatake, *J. Magn. Magn. Mater.* **177-181**, 337 (1998).

[2] B. Gorshunov, P. Haas, O. Ushakov, M. Dressel, F. Iga, *Phys. Rev. B* **73**, 045207 (2006).

[3] N. Sluchanko, L. Bogomolov, V. Glushkov, S. Demishev, M. Ignatov, Eu. Khayrullin, N. Samarin, D. Sluchanko, A. Levchenko, N. Shitsevalova, K. Flachbart, *Phys. Status Solidi B* **243**, R63 (2006).

[4] K. Flachbart, S. Gabáni, K. Gloos, M. Meissner, M. Opel, Y. Paderno, V. Pavlík, P. Samuely, E. Schuberth, N. Shitsevalova, K. Siemensmeyer, P. Szabó, *J. Low Temp. Phys.* **140**, 239 (2005).

[5] H. Weng, J. Zhao, Zh. Wang, Zh. Fang, Xi Dai, *Phys. Rev. Lett.* **112**, 016403 (2014).

[6] F. Iga, S. Hiura, J. Klijn, N. Shimizu, T. Takabatake, M. Ito, Y. Matsumoto, F. Masaki, T. Suzuki, T. Fujita, *Physica B* **259-261**, 312 (1999).

[7] K.S. Nemkovski, P.A. Alekseev, J.-M. Mignot, E.A. Goremychkin, A.A. Nikonov, O.E. Parfenov, V.N. Lazukov, N.Yu. Shitsevalova, A.V. Dukhnenko, *Phys. Rev. B* **81**, 125108 (2010).

[8] N.E. Sluchanko, A.V. Bogach, V.V. Glushkov, S.V. Demishev, K.S. Lyubshov, D.N. Sluchanko, A.V. Levchenko, A.B. Dukhnenko, V.B. Filipov, S. Gabáni, K. Flachbart, *JETP Lett.* **89**, 256 (2009).

[9] N.E. Sluchanko, A.N. Azarevich, A.V. Bogach, V.V. Glushkov, S.V. Demishev, M.A. Anisimov, A.V. Levchenko, V.B. Filipov, N.Yu. Shitsevalova, *J. Exp. Theor. Phys.* **115**, 509 (2012).

[10] A.V. Bogach, N.E. Sluchanko, V.V. Glushkov, S.V. Demishev, A.N. Azarevich, V.B. Filippov, N.Yu. Shitsevalova, A.V. Levchenko, J. Vanacken, V.V. Moshchalkov, S. Gabani, K. Flachbart, *J. Exp. Theor. Phys.* **116**, 838 (2013).

[11] P.A. Alekseev, K.S. Nemkovski, J.-M. Mignot, E.S. Clementyev, A.S. Ivanov, S. Rols, R.I. Bewley, V.B. Filipov, N.Yu. Shitsevalova, *Phys. Rev. B* **89**, 115121 (2014).

[12] V.V. Glushkov, A.V. Kuznetsov, O.A. Churkin, S.V. Demishev, Yu.B. Paderno, N.Yu. Shitsevalova, N.E. Sluchanko, *Physica B* **378-380**, 614 (2006).